Semiclassical Explanation of the Generalized Ramsauer-Townsend Minima in Electron-Atom Scattering

William F. Egelhoff, Jr.
National Institute of Standards and Technology, Gaithersburg, Maryland 20899
(Received 19 February 1993)

The generalized Ramsauer-Townsend minima which occur, at certain scattering angles, in the intensity of electrons elastically scattered by atoms have been a subject of interest in atomic physics for over sixty years. While quantum mechanical calculations predict these minima with great accuracy, no clear, simple, intuitively appealing description of the underlying scattering processes has been given. It is shown here for the first time that simple semiclassical calculations provide such a description.

PACS numbers: 34.80.Bm, 34.80.Dp

It was discovered in the earliest days of electron-atom scattering that minima in the cross section for elastic scattering occur at certain electron energies [1]. The minima which were found at low electron kinetic energies (~ 1 eV) for the inert gases were termed the Ramsauer-Townsend effect [2]. A simple explanation of this effect was soon developed, based on a suggestion by Bohr [2]. Bohr suggested that the part of the electron wave that enters the atom is accelerated by the atomic potential to an extent that just fits an additional integral number of electron wavelengths into the atomic diameter (a phase shift of $2\pi n$). The scattered part of the wave emerging from the atom is thus in phase with the spatially adjacent unscattered part of the wave. This constructive interference means that almost no intensity is removed from the incident beam, and the cross section for elastic scattering appears to be nearly zero [2,3].

At higher energies (e.g., 100–1000 eV) minima were observed at certain scattering angles for the heavier inert gases and metal vapors [2], but no simple explanation was apparent. Suggestions were made that these minima, which in recent years have come to be known as *generalized* Ramsauer-Townsend minima, might be explained if, at certain electron energies, the scattered electron wave were dominated by a single partial wave [2]. This idea may be understood by noting that in the quantum mechanical treatment the asymptotic form of the scattered wave is [2]

$$\Psi = r^{-1} e^{ikr} f(\theta) ,$$

where the scattering amplitude

$$f(\theta) = (2ik)^{-1} \sum_n (2n+1)[\exp(2i\eta_n) - 1] P_n(\cos\theta) ,$$

with η_n the partial-wave phase shift of the nth partial wave and θ the scattering angle. Thus, the angular variation of the intensity is proportional to the square of a spherical harmonic if a single partial wave dominates [2],

$$I(\theta) \approx \text{const} \times \{P_n(\cos\theta)\}^2 .$$

The simple predictions made by this model did not give a very good fit to the data (see Fig. 5.14 in Ref. [4]). A large part of the problem was that in most cases it was clear that a number of partial waves were making important contributions to the scattering amplitude [2]. Quantum mechanical calculations made this fact quite clear and were also able to predict the observed angular distributions accurately [2,4,5]. However, in the quantum mechanical treatment, the sum of amplitudes of the important partial waves yielded a total scattered wave with a complexity that defied a simple, intuitively appealing explanation of the generalized Ramsauer-Townsend minima [6]. Nevertheless, the single-dominant-partial-wave idea was passed down over the decades [4,5], largely unimproved upon, in spite of its obvious shortcomings.

Figure 1 presents a typical example of the generalized Ramsauer-Townsend minima [6–9]. At the lower kinetic energies, various minima are observed as a function of scattering angle in the magnitude of the scattering ampli-

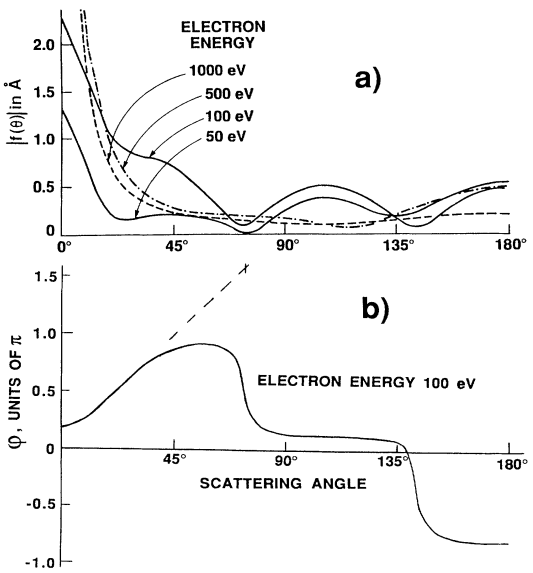

FIG. 1. Plots of (a) the magnitude of the quantum mechanical scattering amplitude, and (b) the phase shift for an electron plane wave scattered by a Cu atom at the indicated electron kinetic energies (from Ref. [7]).

tude, $|f(\theta)|$. [Defined as $f(\theta)=|f(\theta)|e^{i\varphi(\theta)}$, where $\varphi(\theta)$ refers to the phase shift of the full wave [7–9]. Note the distinction that η_n, above, is a partial-wave phase shift for the nth partial-wave basis function.]

Two important characteristics of this effect are that the minima have some tendency to be a periodic function of angle and that the minima fade away at higher electron kinetic energies. Also noteworthy is that, for a given electron kinetic energy, the heavier the atom the greater the number of minima that appear (not illustrated). These general characteristics can be seen clearly if one consults the comprehensive numerical tabulations of the effect found in Refs. [7–9].

Another characteristic of the effect is that as $|f(\theta)|$ goes through a minimum, a rather sudden change in the full-wave phase shift, $\varphi(\theta)$, of approximately π [6–9], occurs. Moreover, the more closely the minimum in $|f(\theta)|$ approaches zero, the more closely the change in the phase shift approaches π [7–9]. Any model intending to explain the generalized Ramsauer-Townsend effect should be able to account for these salient characteristics. As we shall see, even a very simple semiclassical model does so.

Figure 2(a) illustrates two families of electron trajectories obtained from a simple, WKB-level semiclassical calculation [10], using a realistic potential for Cu [11]. These results illustrate the important semiclassical concepts that, first, the closer the electron comes to the nucleus the larger the scattering angle; second, the higher the electron kinetic energy the closer it must come to the nucleus to be scattered through a given angle; and, third, at lower energies and small impact parameters the trajectory can loop around the atom, scattering through, as it were, more than 180° of total deflection. This looping-around effect becomes very weak for light atoms or at high electron kinetic energies, for which the largest scattering angle is near 180° (the Coulomb limit). The looping around is a consequence of the atomic potential varying faster than $1/r$, as the electron descends through the screening shells, and Z_{eff} rises. For heavier atoms, with many electrons screening the nucleus, the looping-around effect is more pronounced. As we shall see, this looping around is the key to understanding all the salient characteristics of the generalized Ramsauer-Townsend effect.

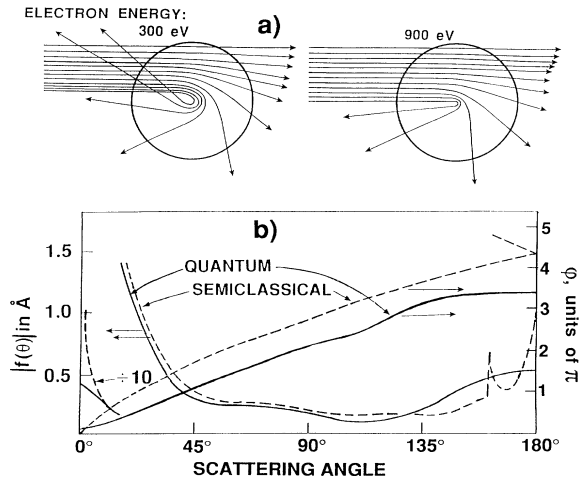

FIG. 2. Plots of (a) two families of semiclassical trajectories for an electron plane wave of the indicated kinetic energy scattered by a Cu atom, and (b) a comparison of the quantum mechanical (from Ref. [7]) and semiclassical (this work) values for the magnitude of the scattering amplitude and phase shifts for a 500 eV electron plane wave scattered by a Cu atom.

Figure 2(b) illustrates the degree to which a simple, WKB-level semiclassical calculation [10], using a realistic potential for Cu [11], reproduces the full quantum mechanical result. While the numerical accuracy is not extremely high, it is adequate to serve as a basis for a qualitative description and explanation of the generalized Ramsauer-Townsend effect. Moreover, more complex semiclassical methods incorporating wave-packet spreading are well established [12], and would give the same qualitative results with increased numerical accuracy. (Note that a minimum uncertainty wave packet with a FWHM of 0.5 Å and a kinetic energy of 500 eV will spread only 9% during the time it takes to travel 2.55 Å, a distance corresponding to the diameter of a Cu atom [13,14].)

The semiclassical $|f(\theta)|$ in Fig. 2(b) is the sum, over all trajectories j leading to the same θ, of the square root of the differential scattering cross section,

$$|f(\theta)|=\left|\sum_j\left(\frac{d\sigma}{d\Omega}\right)_j^{1/2}\exp(i\varphi_j)\right|, \tag{1}$$

where

$$\frac{d\sigma}{d\Omega}=\frac{b}{\sin\theta}\left(\frac{d\theta}{db}\right)^{-1},$$

φ_j are the phase shifts of individual trajectories, and b is the impact parameter. Equation (1) is well established as the semiclassical analog of the quantum mechanical $|f(\theta)|$ [15,16]. The values for $|f(\theta)|$ and $\varphi(\theta)$ in Fig. 2(b) were calculated using well-established methods (see Refs. [15,16]) from families of semiclassical trajectories [e.g., Fig. 2(a) illustrates two such families]. [Such a family provides both the φ_j values and the deflection function, $d\theta/db$, as input for Eq. (1).] Equation (1) may be viewed as relating an areal cross section $d\sigma=2\pi b\,db$ to a solid angle $d\Omega=2\pi\sin\theta d\theta$ [15]. Note three singularities in the semiclassical $|f(\theta)|$ not present in the quantum mechanical $|f(\theta)|$. The ones at 0° and 180° are generic due to the sine term in Eq. (1), and the one at 160° (particular to this case) is due to a zero in the deflection function (a rainbow effect) as the looping around reaches a maximum. (With decreasing b, the looping around effect reaches a maximum deflection then

comes back to 180° for extremely small impact parameters, as it must since the Coulomb limit applies whenever all the important scattering occurs inside the screening shells.) Singularities such as these tend to be smoothed out when wave-packet spreading is included in a calculation and so do not appear in the quantum mechanical result [12,16].

Figure 3 illustrates what the present semiclassical calculations reveal is occurring at the generalized Ramsauer-Townsend minima. Two trajectories passing around opposite sides of the atom and exiting at the same angle are illustrated in Fig. 3(a). The interference between these two is illustrated in Fig. 3(b) as a sum of vectors in the complex plane. With increasing scattering angle, the trajectory labeled 1 in Fig. 3(a) experiences an increase in phase shift, illustrated as the increasing phase angle from vector *a* to vector *b* in Fig. 3(b). Concurrently, for the same increase in *net* scattering angle the trajectory labeled 2 in Fig. 3(a) experiences a decrease in phase shift, illustrated as the decreasing phase angle from vector *c* to vector *d* in Fig. 3(b). This decrease is a result of the *total* scattering angle for this looping-around trajectory being less for the larger *net* scattering angle. Note in the semiclassical phase shift of Fig. 2(b), where only a single trajectory is considered, the phase shift rises roughly linearly even beyond 180° [note this part of the plot is folded back at the top right corner in Fig. 2(b)].

In Fig. 3(b) it is apparent that, with increasing *net* scattering angle, the vectors corresponding to trajectories 1 and 2 are counterrotating, and as they go through a phase difference of π, their sum both goes through a minimum and exhibits a sudden change in phase of π (vectors *e* to *f*). This phenomenon is the basis of the generalized Ramsauer-Townsend minima, and the wide applicability of these simple principles can be noted by studying the comprehensive numerical tabulations of the effect found in Refs. [7–9]. Somewhat similar phenomena occur in atom-atom [15], ion-atom [17], and atom-electron scattering [18], and perhaps in muon-atom scattering [19].

A typical example of this applicability may be illustrated using the 100 eV data of Fig. 1. In Fig. 1(b) the phase shift exhibits two sudden changes, each of almost π, at just the angles for which minima occur in $|f(\theta)|$,

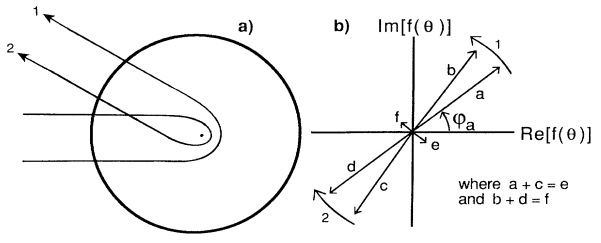

FIG. 3. Illustrations of (a) the two basic types of trajectories needed to explain the generalized Ramsauer-Townsend minima, and (b) how the interference between them can be represented as the sum of two vectors in the complex plane.

74° and 144°. Figure 4 illustrates how this effect may be explained qualitatively [20], using the concepts of Fig. 3, for six key values of θ. It may be easiest to start by considering Fig. 4(c), which at $\theta=80°$ is just beyond the 74° minimum in $|f(\theta)|$. Note first that if the initial slope (which should be dominated by a type 1 trajectory) in Fig. 1(b) is extrapolated (dashed line) to 74°, a phase shift of $\sim 1.6\pi$ is predicted for the type 1 trajectory. This value suggests that the looping-around (type 2) trajectory (which must be π out of phase to create the minimum) will have a phase shift of $\sim 0.6\pi + 2\pi n$, where n is an integer. These vectors are plotted in Fig. 4(c). The fact that the change in the phase shift near 74° is somewhat less than π consistent with the fact that $|f(\theta)|$ [in Fig. 1(a)] does not go exactly to zero. This simply means the two vectors are somewhat unequal in length. Continuing to larger scattering angle in Fig. 1(b), little change is seen in the phase shift as $|f(\theta)|$ goes through a maximum around 106°. This constructive interference effect, illustrated in Fig. 4(d), is simply a consequence of the vectors continuing to precess at a similar rate in a counterrotating sense. The similar rate indicates that, as in the semiclassical phase shift of Fig. 2(b), the phase shift rises roughly linearly even beyond 180° as the trajectories loop around the atom. As the vectors continue their counterrotation at this rate, they interfere destructively near 144° [see Fig. 4(e)], and here the phase shift again changes by nearly π. Finally, at 180° the vectors add constructively, as they must, since in the limit at 180° there is no difference between the two types of trajectories [see Fig. 4(f)]. Figures 4(a) and 4(b) can be understood by working backwards from 4(c) using the above arguments. The slight dip in $|f(\theta)|$ around $\theta=30°$ in Fig. 1(a) suggests that the type 2 trajectory is starting to contribute (~out of phase), and this effect is represented in Fig. 4(a).

Note how this description makes the connection between a roughly linear relationship between phase shift and scattering angle for the semiclassical trajectories and the roughly periodic constructive-destructive behavior (as a function of scattering angle) in the generalized Ramsauer-Townsend effect. This approximate periodici-

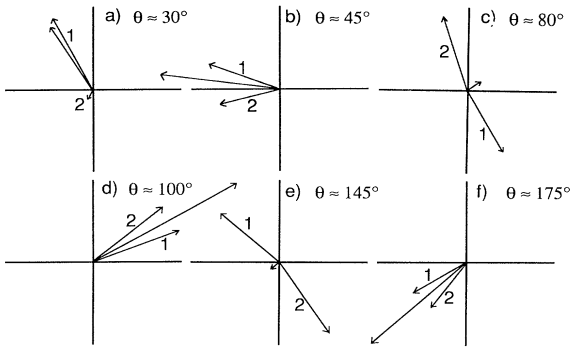

FIG. 4. An explanation of the 100 eV data of Figs. 1(a) and 1(b) in terms of the model illustrated in Fig. 3.

ty in scattering angle is one of the most striking characteristics that one observes in studying the comprehensive numerical tabulations of the effect found in Refs. [7–9]. It is particularly noticeable for the heavier atoms at electron energies of a few hundred eV where as many as four periodic minima [and their attendant changes in $\varphi(\theta)$ of $\sim\pi$] can be observed (e.g., Au at 500 eV).

Note that at the higher energies the semiclassical model also explains the gradual disappearance of the enhances backscattering around 180° [e.g., from 500 to 1000 eV in Fig. 1(a)]. When the looping around ceases, a constructive interference between two trajectories is no longer possible.

An interesting example of the absence of generalized Ramsauer-Townsend minima is found in positron-atom scattering in which the strongly repulsive potential cannot induce looping-around trajectories. A very instructive comparison of $|f(\theta)|$ plots for electron and positron scattering from Cu at 100 eV may be found in Fig. 1 of Ref. [21].

In summary, the salient features of the generalized Ramsauer-Townsend effect for electron energies of a few hundred eV or more are readily accounted for by a very simple semiclassical description. The only regime in which this interpretation seems to fail is that of low electron kinetic energies, where a semiclassical description is not expected to be valid, due to rapid spreading of small wave packets, and indeed at low energies minima periodic in angle and sudden changes in phase shift of $\sim\pi$ are not generally observed. The description appears to be valid for heavy atoms such as Au at electron kinetic energies as low as 250 eV, and for lighter atoms such as Cu at electron energies as low as 100 eV. While a WKB-level treatment is excellent for illustrating the basic principles of this effect, it cannot be expected to simulate experimental data with great numerical accuracy. For that, improvements such as wave-packet spreading would be needed [12]. However, if numerical accuracy, rather than understanding, is the goal then a full quantum mechanical treatment is best.

It is interesting to reflect on the reasons why it took so long for this simple, clear, and intuitively appealing explanation of a familiar problem in physics to be recognized. The data, and the semiclassical concepts needed to understand it, have been well known to the physics community for over sixty years. One can only conclude that it was a preoccupation with the partial-wave basis set of the quantum mechanical treatment which delayed the recognition of the present understanding for so long. It is commonplace that, in problems of physics, the choice of basis set can be the key to understanding. In the present case, families of semiclassical trajectories constitute the most informative basis set. This result illustrates the great value of semiclassical models in providing insights which, in quantum mechanical models, may be hopelessly obscured or lost in complexity.

The author wishes to thank Professor S. M. Girvin and Dr. J. W. Gadzuk for several valuable discussions in the early stages of this work and D. Barak for help with the calculations.

[1] C. W. Ramsauer, Ann. Phys. (Leipzig) **64**, 513 (1921); **66**, 545 (1921); J. S. Townsend and V. A. Bailey, Philos. Mag. **43**, 593 (1922); R. Kollath, Phys. Z. **31**, 985 (1931).

[2] N. F. Mott and H. S. W. Massey, *The Theory of Atomic Collisions* (Oxford Univ. Press, Oxford, 1933).

[3] See S. Geltman, *Topics in Atomic Collision Theory* (Academic, New York, 1969), pp. 23–26.

[4] H. S. W. Massey, *Atomic and Molecular Collisions* (Taylor & Francis, London, 1979), pp. 68–86.

[5] H. S. W. Massey and E. H. S. Burhop, *Electronic and Ionic Impact Phenomena* (Oxford Univ. Press, Oxford, 1952), pp. 123–137.

[6] J. J. Barton and D. S. Shirley, Phys. Rev. B **32**, 1892 (1985).

[7] M. Fink and A. C. Yates, At. Data **1**, 385 (1970).

[8] M. Fink and J. Ingram, At. Data **4**, 1 (1972).

[9] D. Gregory and M. Fink, At. Data **14**, 39 (1974).

[10] Following the methods of A. P. Jauho, J. W. Wilkins, M. Cohen, and R. P. Merrill, in *Determination of Surface Structure by LEED*, edited by P. M. Marcus and F. Jona (Plenum, New York, 1985), p. 129.

[11] V. L. Moruzzi, J. F. Janak, and A. R. Williams, *Calculated Electronic Properties of Metals* (Pergamon, New York, 1978).

[12] E. Heller, J. Chem. Phys. **62**, 1544 (1975); **75**, 2923 (1981).

[13] See C. Cohen-Tannoudji, B. Diu, and F. Laloë, *Quantum Mechanics* (Wiley, New York, 1977), Vol. 1, p. 64.

[14] It may be noted that in Fig. 2(a) the trajectories leading to large-angle scattering pass closer than 0.5 Å of the nucleus. This is not a problem because at the turning point, deep within the atom, the electron has a kinetic energy of a few keV so that in these cases a much smaller minimum-uncertainty wave packet could be used without undue spreading.

[15] R. B. Bernstein, Adv. Chem. Phys. **10**, 75 (1966).

[16] M. V. Berry and K. E. Mount, Rep. Prog. Phys. **35**, 315 (1972).

[17] R. L. Champion, L. D. Doverspike, W. G. Rich, and S. M. Bobbio, Phys. Rev. A **2**, 2327 (1970).

[18] D. R. Schultz and R. E. Olson, J. Phys. B **24**, 3409 (1991).

[19] P. Kammel, in *Muonic Atoms and Molecules*, edited by L. A. Schuller and C. Petetijean (Birkhäuser-Verlag, Basel, 1993), p. 115 [Fig. 3(b)].

[20] The approximation used to construct Fig. 4 [and make it agree almost perfectly with Fig. 1(b)] was that the phase-shift rises by π every 46° for $\theta=0°$ to 100° and by π every 72° for $\theta>100°$. A determination of which of the two vectors is longer at the destructive condition can be made by noting whether the change in phase shift of $\sim\pi$ is an increase (i.e., type 1 longer) or a decrease (i.e., type 2 longer).

[21] S. Y. Tong, H. Huang, and X. Q. Guo, Phys. Rev. Lett. **69**, 3654 (1992).